WIND-TUNNEL SIMULATION OF THE THERMALLY STRATIFIED ATMOSPHERIC BOUNDARY LAYER IN COMPLEX TERRAIN

Kuznetsov S.[1]*, Pospíšil S.[1], Michalcová V.[2] and Kozmar H.[3]
*Author for correspondence
[1]Centre of Excellence Telč, Institute of Theoretical and Applied Mechanics,
Prosecká 76, 190 00 Prague, Czech Republic,
E-mail: kuznetsov@itam.cas.cz, pospisil@itam.cas.cz
[2]Department of Mechanics, Faculty of Civil Engineering, Technical University Ostrava
L. Podéště 1857, 182 00 Ostrava, Czech Republic,
E-mail: vladimira.michalcova@vsb.cz
[3]Faculty of Mechanical Engineering and Naval Architecture, University of Zagreb,
Ivana Lučića 5, 10000 Zagreb, Croatia,
E-mail: hkozmar@fsb.hr

ABSTRACT

Some characteristics of thermal effects in wind-tunnel simulations of the atmospheric boundary layer (ABL) flow developing above hill terrain are discussed in the paper. Particle image velocimetry (PIV) analysis and its numerical validation of the convective ABL developing above the heated hill obstacle are presented. The differences and instable stratification effects between the windward and leeward sides of a hill model were investigated for different wind characteristics. Particularly, the buoyancy effects on the structure of the ABL simulation in a wide range of stability conditions expressed by Richardson number are studied. The stratification was modeled in the Vincenc Strouhal climatic wind tunnel of the Institute of Theoretical and Applied Mechanics of the Czech Academy of Science.

INTRODUCTION

Wind climate influencing wind loads on buildings and other structures, as well as dispersion of pollutants from various surface is essentially determined by small-scale motions and processes occurring in the atmospheric boundary layer (ABL), also known as the planetary boundary layer (PBL). The physical and thermal properties of the underlying surface, in conjunction with the dynamics and thermodynamics of the lower atmosphere (troposphere), determine ABL depth and its characteristics. The most important factors determining the wind distribution in a fair-weather ABL are the large scale horizontal pressure and temperature gradients (alternatively, geostrophic and thermal winds), the surface friction and roughness characteristics, the Earth's rotation, thermal stratification caused by the diurnal heating and cooling cycle, and entrainment at the top of the ABL. Both the magnitude and direction of horizontal velocity vary with height in response to the Coriolis and friction (shear) forces. Atmospheric turbulence is characterized by high degree of irregularity, three-dimensionality, diffusivity, dissipation, and a wide range of motion scales.

NOMENCLATURE

g	[m/s^2]	Acceleration of gravity
H	[m]	Height of the hill
h	[W/(m^2·K)]	Convective heat transfer coefficient of the flow
k	[W/(m·K)]	Thermal conductivity of the flow
L	[m]	Characteristic length
K	[m^2/s]	Coefficient of turbulent diffusion
L_{mo}	[mm]	Monin-Obukhov stability length
Re	[-]	Reynolds number
Ri	[-]	Richardson number
T	[°C]	Temperature of the warm surface
T_o	[°C]	Reference temperature
Q	[kW]	Energy of the heating
u_*	[-]	Friction (shear) velocity
$V(z)$	[m/s]	Mean wind speed at height z
V_0	[m/s]	Reference wind velocity
x	[m]	Distance in longitudinal direction
y	[m]	Distance in lateral direction
z	[m]	Distance in vertical direction
z_o	[m]	Aerodynamic surface-roughness length
z_s	[m]	Atmospheric surface layer with a height

Special characters

α	[m^2/s]	Thermal diffusivity
β	[-]	Generalized wind profile exponent, $\beta=\beta(Ri)$
κ	[-]	Von Karman constant is
ν	[m^2/s]	Kinematic viscosity of air
ρ	[kg/m^3]	Density of air
τ_o	[kg/m^2]	Mean surface shear stress
Θ	[K]	Absolute temperature ($\Theta=T+273$°C)

Following the original suggestion of Reynolds, it is common to consider various variables in a turbulent flow as sums of their mean and fluctuating values. Almost all turbulence theories and models are semi-empirical because of the fundamental problems and difficulties encountered in purely mathematical description of turbulence. In the fully-developed isothermal (indifferent thermal stratification) homogeneous surface layer above the canopy or roughness layer, the momentum flux is nearly constant with height and directly related to the surface shear stress. An appropriate similarity hypothesis, verified by experimental data, is that the

mean velocity gradient and turbulent quantities depend only on the height above the surface, and the kinematic momentum flux or surface shear stress. The surface roughness parameter is found to be strongly dependent on the average height of roughness elements and, to a lesser extent, on their spacing density and aerodynamic characteristics.

In many engineering applications, modelling conditions with strong winds are especially important. It is usually assumed that the influence of heat convection can be disregarded. In such cases, logarithmic profiles prevail for wind speed and scalars; variances of the wind components are essentially constant with height, and velocity spectra have relatively simple properties. The limits to which these "mechanical" approximations are adequate depend on many factors such as wind speed, roughness, heat flux, and height. In reality, the ABL nearly always has some vertical heat flux either in the form of sensible or latent heat. The larger the height, the more important convection becomes. Also, the strength of convection increases with vertical flux of heat (to which a moisture term must be added under hot, cold, humid conditions). Dependent on whether the heat flux is upward (unstable) or downward (stable), in addition to the mechanical production; turbulent energy is either produced or dissipated. Consequently, the mean flows, as well as turbulence in the adiabatic surface layer, differ from those in the neutrally stratified surface layer and the modification of mean wind profile and fluctuation needs to be taken into account. In another words, stability and stratification characteristics are important. For example, they play a major role in the pollutant diffusion problems in the real atmosphere, and often, the very hazardous environmental and wind-loading conditions are a direct result of those effects.

The models of the thermally stratified surface layer of the atmosphere proposed by Monin and Obukhov are based on a general similarity hypothesis in which the kinematic heat flux and the buoyancy are accounted for. Generally, the mean wind speed increases with height, at least in the lower-half of the ABL, while the mean wind direction may also change with increasing height due to Coriolis force effects. The wind speed distribution in the surface layer is given by the similarity relation for the quantitative expression for the development of turbulent and convective motion in the boundary layer called Monin-Obukhov length. Physically, the Monin-Obukhov length is equal to the height where there is a balance between mechanically produced and thermally dissipated turbulence at the stable thermal stratification.

In [1], the measured vertical profiles are studied with respect to the modification of the logarithmic wind profiles. Several researchers have investigated in detail the wind flow over generic topographic terrain using various experimental techniques. The flow field over generic escarpments and conical hills were determined [2, 3] using CTA measurements. Surface pressure measurements and the flow visualizations [4], as well as CTA and Pitot tube measurements for isolated two-dimensional hills were performed in [5]. The rough estimates of the effect of a small hill on wind characteristics are presented analytically in [6]. CTA and PIV mixed measurements were performed in [7] for isolated valleys. Thermal effects on the airflow, building geometry and architecture as well as street canyon dimensions, have been mainly studied using wind-tunnel experiments [8, 9, 10, 11] and numerical models [12, 13, 14] and fewer with full-scale or near full-scale experiments [15, 16]. The mass transfer from street canyon surfaces by a naphthalene sublimation technique in a wind tunnel was investigated [17]. This technique was used to quantify scalar vertical fluxes out of a street canyon under neutral conditions. The convective transfer velocity from individual wall surfaces was evaluated in an urban canyon using a water evaporation technique [18].

The authors present the wind-tunnel experiments focused on the low turbulent flows within the instable and indeterminate thermal stratification. The convective boundary layer is created with the convective turbulent natural flow developing as the complex ground model (hill) is warmed up, e.g., by the solar radiation. The flow is analysed with respect to its stability expressed by the Richardson number. The flow data are obtained using Particle Image Velocimetry (PIV) method and compared with the computational analysis for validation. Also, the constant temperature anemometry (CTA) experiments were carried out in order to distinct the contributions of thermally and mechanically induced atmospheric turbulence. These results, however, together with stable stratification models, will be analysed in future studies.

WIND-TUNNEL EXPERIMENTS

Wind-tunnel experiments were carried out in the closed-circuit Vincenc Strouhal climatic wind tunnel (CWT) of the Centre of Excellence Telč (CET) [19], Czech Republic (http://cet.arcchip.cz). This wind tunnel is designed to determine wind effects on structures, aero-elastic structural response, ABL modelling, and other civil, mechanical, and environmental engineering applications. It consists of an aerodynamic section, a climatic section, a fan section, and heating/cooling exchanger. The aerodynamic section of the wind tunnel is 1.9 m wide, 1.8 m high and 11 m long rectangular cross-section with a possibility to regulate airflow velocity from 0.06 m/s to 50 m/s. The method used to simulate the ABL is a variation of the method employed by Counihan [20, 21]. There are three main components: castellated barrier wall, elliptical wedge vortex generators, and surface roughness elements. The coordinate system is defined with x in the stream-wise direction, z in the wall-normal direction, and y in the span-wise direction.

The hill model with the height H=200 mm was inserted into the testing chamber (see Figure 1). The model of the hill is made modularly from six heating elements. The lower surfaces of models were covered with heat insulation. The velocity values are selected for the perpendicular wind direction to the long side of the hill. Heating of the hill was produced by individual electrical heating elements with sepaprated control. Produced energy sufficed to heat a boundary layer approximatelly 300 mm thick, which is from 5 to 10 times the depth of the anticipated model-scale Monin-Obukhov stability length, L_{mo} = 30-60 mm. The wind velocity during the experiments ranged from 0 m/s up to 5 m/s and the temperature

was in the interval from 20 ºC up to 200 ºC. Some of the selected examples are presented.

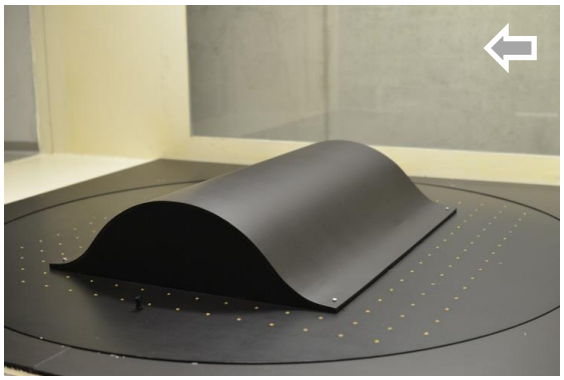

Figure 1 Model a heated hill obstacle in the wind tunnel

The lower portion of the neutrally stratified ABL (above the flat surface) where turbulent fluxes vary within about 10 % is defined as the atmospheric surface layer with a height z_s. Mean velocity profiles in the boundary layer are given by the well-established logarithmic distribution:

$$V(z) = \left(\frac{u_*}{\kappa}\right) \cdot \ln\left(\frac{z}{z_0}\right). \quad (1)$$

In the full-scale ABL, the logarithmic law is not satisfactory when in the lower layer exist non-zero vertical temperature gradient. Mean velocity profiles in the thermally stratified ABL developing above flat terrain are given as the modification of the Eq. (1).

$$\frac{\partial V}{\partial z} = \left(\frac{u_*}{\kappa \cdot z_o}\right) \cdot \left(\frac{z}{z_o}\right)^{-\beta}. \quad (2)$$

Using the coefficient β, which is dependent on the Richardson number (*Ri*) given by the equation

$$Ri = \frac{g}{\Theta} \frac{\partial \Theta / \partial z}{(\partial V / \partial z)^2}, \quad (3)$$

the thermal stratification correction of the wind profile is included. This can be obtained from the Eq. (2) after the integration with respect to vertical coordinate *z*:

$$V(z) = \left(\frac{u_*}{\kappa(1-\beta)}\right) \cdot \left[\left(\frac{z}{z_0}\right)^{1-\beta} - 1\right]. \quad (4)$$

Value of β decreases with increasing *Ri*. For β=1 the integration of Eq. (3) leads to the logarithmic profile in Eq. (1). Anyway, the simulation of the stratified ABL requires geometric similarity of surface roughness, dynamic similarity of inertial and buoyancy forces, and similarly distributed mean and turbulent upwind velocity and temperature profiles. Viscous and Coriolis forces are not expected to dominate: hence, equivalence of model and prototype Rossby and Reynolds numbers are not required, while the equivalence between Richardson numbers is essential. Obviously, the flow over the hill, as it is in this case, is far from being governed by the logarithmic law, so it is impractical to discuss the results with one coefficient only, which is moreover usefull for the flow over the less complex terrain. Therefore, for presented experiments, the analysis of Richardson (*Ri*) numbers and the local flow instabilities is carried out. The leeward zone of the hill is divided into three regions: outer region above the top of the hill, intermittent zone at the level of the hill top, and the inner region between the ground surface and the hill top, see the blue band in Figs. 6-10.

PIV experiments, flow fields

PIV experimental equipment from Dantec and Litron Lasers was used. A Dantec FlowSense EO camera captured the snapshots of the flow-field. Its resolution is 2048 × 2048 pixels. A pulsed Nd-YAG laser illuminated the flow. The flow was seeded using a fog generator. The fog generator was activated for a few seconds in the climatic section, and then deactivated. After some time, the smoke dispersed and resulted in a homogeneously seeded flow field.

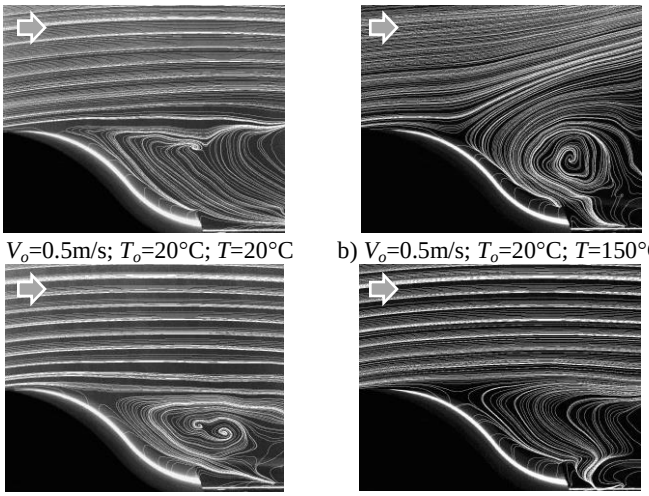

a) V_o=0.5m/s; T_o=20°C; T=20°C b) V_o=0.5m/s; T_o=20°C; T=150°C

c) V_o=1.5m/s; T_o=20°C; T=20°C d) V_o=1.5m/s; T_o=20°C; T=150°C

Figure 2 Convective trajectories and the mixing of the natural convective flow and forced convective flow

A series of 50 double pictures at a rate of 10 Hz was recorded. The time between a pair of images was 4000 μs. The Reynolds number in the PIV experiment was $Re \approx 5 \cdot 10^3$. The images were analysed using Dantec Dynamic Studio (version 3.31) software. The adaptive correlation technique was chosen to obtain the local flow velocity. A final interrogation area size of 32 pixels with three iteration steps was set. The resulting vector field was smoothed using a 3 × 3 moving average filter. The whole hill model was heated. The reference velocities were V_0 = 0.5 m/s; 1.5 m/s and 5 m/s respectively. The hill temperature was selected to be T = 20°C, 50°C, 100°C, 150°C and 200 °C, the reference temperature of the air flow was T_0 = 20 °C. The mean streamlines are shown for selected cases in Fig. 2.

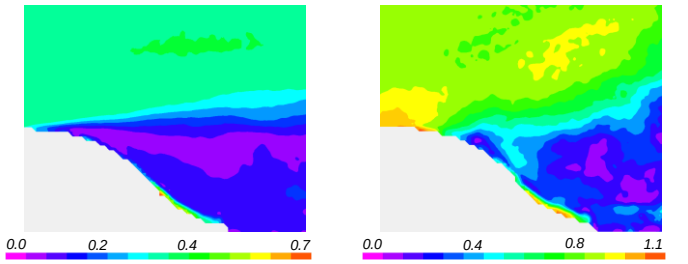

a) V_o=0.5m/s; T_o=20°C; T=20°C b) V_o=0.5m/s; T_o=20°C; T=150°C

c) V_o=1.5m/s; T_o=20°C; T=20°C d) V_o=1.5m/s; T_o=20°C; T=150°C

Figure 3 Experimental velocities

Computational simulation

Thermally stratified ABL was previously numerically studied in [22, 23, 24]. There, transition of the initial flow with the low turbulence into the fully developed turbulent flow behind a heated hill is simulated. In the present study, the computational simulations are performed using Ansys Fluent and the SST k-ω turbulence model [25].

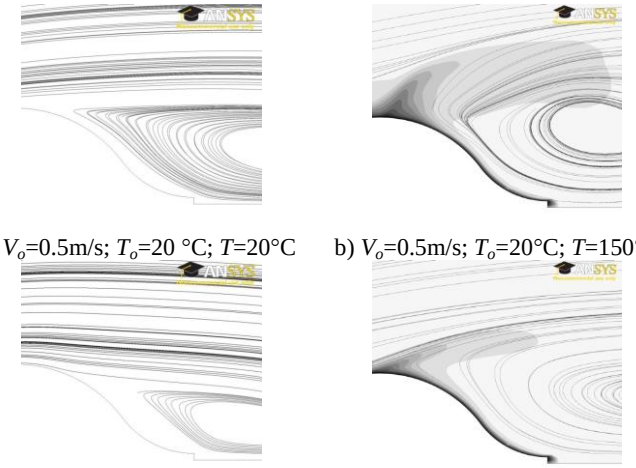

a) V_o=0.5m/s; T_o=20 °C; T=20°C b) V_o=0.5m/s; T_o=20°C; T=150°C

c) V_o=1.5m/s; T_o=20°C; T=20°C d) V_o=1.5m/s; T_o=20°C; T=150°C

Figure 4 Computationally determined streamlines

The standard empirical k-ω model describes well assumed shear flows using two transport equations; for the kinetic energy k and for an energy dissipation parameter ω, respectively. The full Transition SST model is based on two transport equations, one for intermittency and one for the transition onset criteria in terms of momentum thickness Reynolds number. The model is able reflect the difference between low and high turbulence at the border between the wake of the obstacle and the free stream. At the vicinity of the heated object, the buoyancy forces play important role. In this study, a Boussinesq model incorporated in the equation of the thermal transport is used to simulate the natural and forced convection.

FLOW PROFILES, RESULTS, AND DISCUSSION

The extent of thermal stability is described by a similarity parameter Ri in the gradient form. It describes the relative strength of buoyant and inertial forces. Generally, the turbulence and convection develop better for lower Ri. It is immediately observed from the Eq. (3) that under stable thermal stratification ($\delta\Theta/\delta z > 0$) Ri are positive and increase with increasing stability of the thermal stratification and with the increase of the vertical wind shear.

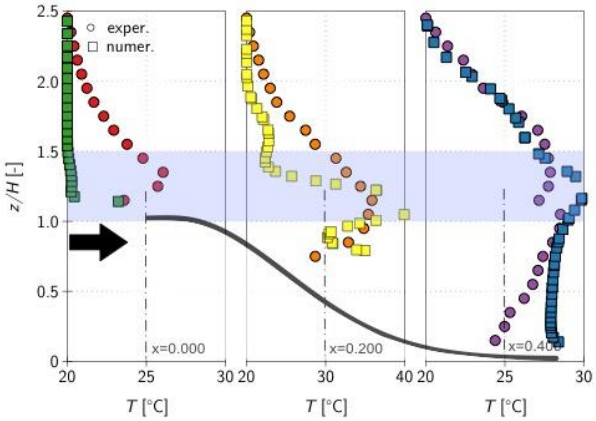

Figure 5 Temperature profiles, V_o=0.5 m/s; T_o=20 °C; T=150 °C

This corresponds to the well known fact, that the stable stratification and the lower wind shear dissipate the mechanical turbulence. The limit case Ri = 1 would lead (under certain assumption about the turbulent diffusion coefficients) to the conclusion, that all the turbulent mechanically-generated kinetic energy is dissipated by the influence of a stable stratification. At indifferent stratification, Ri is zero and at the instable stratification the Ri is negative.

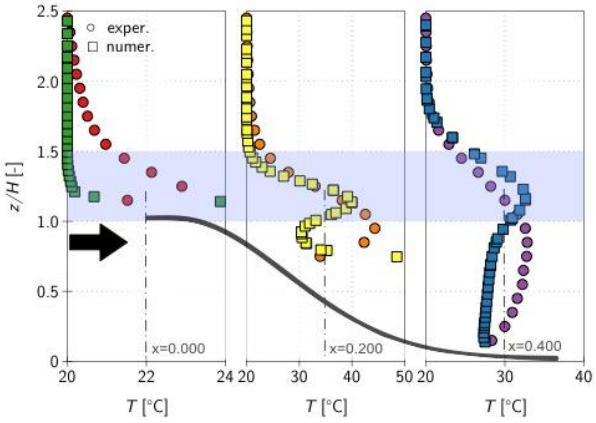

Figure 6 Temperature profiles V_o=1.5 m/s; T_o=20 °C; T=150 °C

If the Ri decreases in the domain of instable stratification, the condition for the turbulent and convective motion improves. Because for the total kinetic turbulent energy balance under the instable stratification the termical production of the turbulence is usually more influencial than the mechanical one, it is much more important to monitor the change of the vertical gradient of

the potential temperature rather than the shear, see Figs. 5 and 6. There, experimental values (circle) are compared to the numerical ones (squares). There is a very good agreement of the results at the leeward side of the hill for the values of distances x = 200 mm, and x = 400 mm from the hill symmetry axis in the alongwind direction. The elevation z is normalized using the height H. In Figs. 7 and 8, the resulting velocity profiles are shown together with the profiles with cold surface (triangles). Without heating, the vertical velocity becomes negative forming a downdraft flow in the lee of the hill.

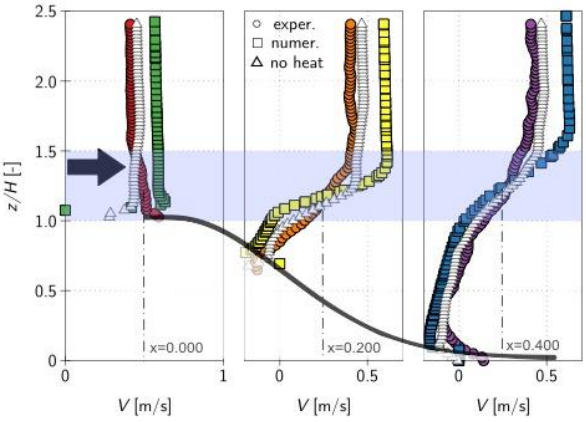

Figure 7 Velocity profiles; V_o=0.5 m/s; T_o=20 °C; T=150 °C

In the case of surface heating, resulting in an upward heat flux, the mechanical turbulence production is augmented with buoyant energy. Near the floor, the mechanical energy production dominates but decreases rapidly with height, while on the other hand the buoyant production is almost constant throughout the surface layer. Outside the surface layer, the flow undergoes vertical mixing due to positive buoyancy forces and the production of large-scale convective turbulence. The vertical component of the velocity shows some variability, see also Fig. 2.

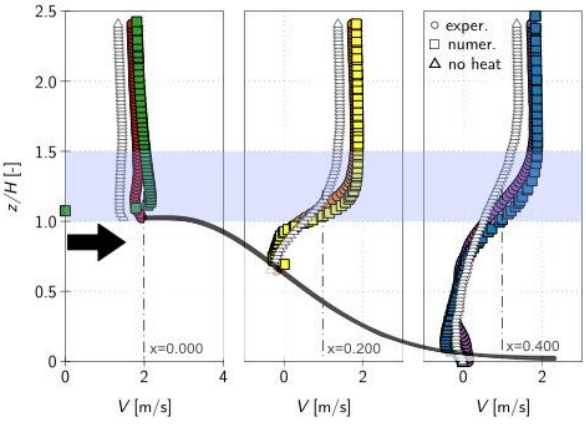

Figure 8 Velocity profiles; V_o=1.5 m/s; T_o=20 °C; T=150 °C

This well-mixed flow, which spans from z/H=2.0 - 2.5, is characterized by an almost uniform potential temperature and by a constant wind speed and direction. In addition, downward fluxes of momentum and heat due to entrainment into the convective boundary layer complicate the flow. Near the surface the turbulent heat and momentum fluxes exist as a result of temperature and velocity gradients, however in the mixed layer, buoyancy effects and entrainment maintain the fluxes. In this layer the fluxes become insensitive to existing gradients and near the top of the surface layer the interaction of the gradient-produced turbulence and buoyancy driven turbulence controls the flow.

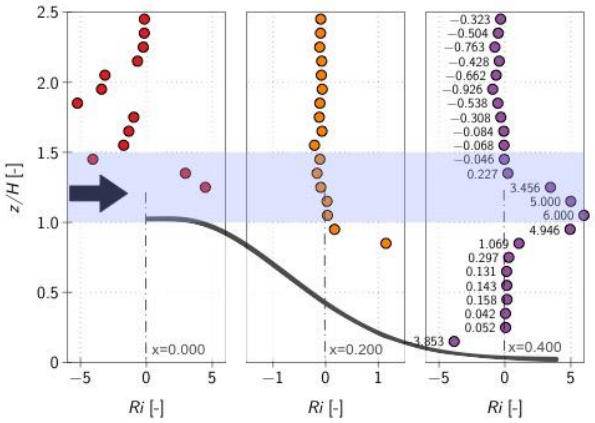

Figure 9 Richardson number; V_o=0.5 m/s; T_o=20 °C; T=150 °C

The criteria for the dynamic stability or instability of a stratified shear layer are given in terms of the wind-profile shape (particularly, the presence of an inflection point) and the gradient Ri. A layer becomes dynamically unstable if the velocity profile has an inflection point and Ri given by Eq. (3) is lower than critical, separating two regimes of stability, the weakly stable and strongly stable. Instability generally leads to an exponential growth of small perturbations or waves in the flow, their breakdown into three-dimensional disturbances and ultimately, to random turbulence. In Fig. 9, Ri is calculated using a numerical version of Eq. (3) for the V = 0.5 m/s. We focus on the downstream distance x = 0.4 m as the place of e.g. potential building site.

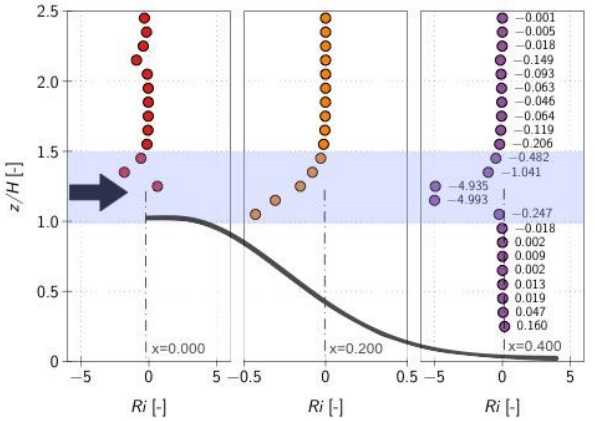

Figure 10 Richardson number; V_o=1.5 m/s; T_o=20 °C; T=150 °C

It can be seen, that Ri is negative in the upper part of the profile, however, in the lower part of the profiles Ri increases and becomes positive, especially in the intermittent region between z/H = 1.0-1.5, where the temperature gradient is positive. This means, that the flow is dynamically stable, because there is on average a stable thermal stratification in that region. Even closer to the surface, Ri is still positive, as the

temperature gradient is positive, but smaller due the higher velocity shear $\partial V/\partial z$. At larger wind speed, Fig. 10, Ri is negative throughout the entire region. The turbulence production is larger as well as the temperature gradient (Fig. 7), which is negative or almost neutral starting from the hill top. There is only inner part of the layer, where $Ri = 0.16$ is near to the critical value $Ri_c = 0.25$, and the production of the turbulence starts to occur. In both experimental cases, Richardson numbers are in the range of estimates of the bulk Ri summarized in [26].

CONCLUDING REMARKS

The experimental wind-tunnel modelling of instable thermal stratification of the ABL developing above a hill is presented. Particularly, the buoyancy effects on the structure of a turbulent boundary layers and the in a wide range of stability conditions were successfully modelled in a wind tunnel. Particle image velocimetry was used for the measurement of flow characteristics around a heated obstacle with a hill shape. The thermal stratification effects on the wind profiles investigation in the leeward side were investigated for two cases of the free stream velocity. Their properties expressed primarily by Richardson number (Ri) were analysed showing, that it is possible to maintain the similarity with respect to the Ri observed in the atmosphere. Future studies will be focused on the analysis of the turbulent patterns obtained by the hot wire anemometry using method of the rotationally slanted wire probe heated to various temperatures at the constant velocity.

ACKNOWLEDGEMENTS

This research was financially supported by the project GAČR No. 14-12892S of the Czech Science Foundation, CET sustainability project LO12 (SaDeCET) and by the Conceptual Development of Science, Research and Innovation for 2016 allocated to the VSB-Technical University of Ostrava, by the Czech Ministry of Education Youth and Sport.

REFERENCES

[1] Deacon, E.L., Vertical diffusion in the lowest layers of the atmosphere, *Quar. J. Royal Meteor. Soc.*, Vol. 75 (323), 1949, pp. 89-103

[2] Bowen A.J., and Lindley D., A wind-tunnel investigation of the wind speed and turbulence characteristics close to the ground over various escarpment shapes, *Boundary-Layer Meteorology*, Vol. 12, 1977, pp. 259-271

[3] Pearse J.R., Wind flow over conical hills in a simulated atmospheric boundary layer, *J. Wind. Eng. Ind. Aerodyn*., Vol. 10, 1982, pp. 303-313

[4] Ferreira A.D., Lopes A.M.G., Viegas D.X., and Sousa A.C.M., Experimental and numerical simulation of flow around two-dimensional hills, *J. Wind. Eng. Ind. Aerodyn.*, Vol. 54/55, 1995, pp. 173-181

[5] Kim H.G., Lee C.M., and Lim H.C., An experimental and numerical study on the flow over two-dimensional hills, *J. Wind. Eng. Ind. Aerodyn*, Vol. 66, 1997, pp. 17-33

[6] Jackson, P.S. and Hunt, J.C.R., Turbulent wind flow over a low hill, *Quarterly Journal of the Royal Meteorological Society*, Vol. 101 (430), 1975, pp. 929-955

[7] Garvey B., Castro I., Wiggs G., and Bullard J., Measurements of flows over isolated valleys, *Boundary-Layer Meteorology*, Vol. 117, 2005, pp. 417-446

[8] Sada K., Wind tunnel experiment of tracer gas diffusion within unstable boundary layer over coastal region, *Atmospheric Environment*, Vol. 36, 2002, pp. 4757-4766

[9] Ohya Y., and Uchida T., Laboratory and numerical studies of the atmospheric stable boundary layers, *Journal of Wind Engineering and Industrial Aerodynamics*, Vol. 104-106, 2008, pp. 379-388

[10] Maruyama Y., Tamura T., Okuda Y., and Ohashi M., LES of turbulent boundary layer for inflow generation using stereo PIV measurement data, *J. Wind. Eng. Ind. Aerodyn*, Vol. 104-106, 2012, pp. 379-388

[11] Pillai S.S., and Yoshie R., Experimental and numerical studies on convective heat transfer from various urban canopy configurations, *J. Wind. Eng. Ind. Aerodyn.*, Vol. 104-106, 2012, pp. 447-45

[12] Kim J., and Baik J., Urban street-canyon flows with bottom heating, *Atmospheric Environment*, Vol. 35, 2001, pp. 3395-3404

[13] Xie X., Liu C.H., and Leung D.Y.C., Impact of building facades and ground heating on wind flow and pollutant transport in street canyons, *Atmospheric Environment*, Vol. 41, 2007, pp. 9030-9049

[14] Qu Y., Milliez M., Musson-Genon L., and Carissimo B., Numerical study of the thermal effects of buildings on low-speed airflow taking into account 3D atmospheric radiation in urban canopy, *J. Wind. Eng. Ind. Aerodyn.*, Vol. 104-106, 2012, pp. 474-483

[15] Kanda M., Progress in the scale modeling of urban climate: review, *Theoretical and Applied Climatology*, Vol. 84, 2006, pp. 23-33

[16] Niachou K., Livada I., and Santamouris M., Experimental study of temperature and airflow distribution inside an urban canyon during hot summer weather conditions. Part II. Airflow analysis, *Building and Environment*, Vol. 43, 2008, pp. 1393-1403

[17] Barlow J.F., Harman I.N., and Belcher S.E., Scalar fluxes from urban street canyons. PartI: Laboratory simulation, *Boundary-Layer Meteorology*, Vol. 113, 2004, pp. 369-385

[18] Narita K., Experimental study of the transfer velocity for urban surfaces with a water evaporation method, *Boundary-Layer Meteorology*, Vol. 122, 2007, pp. 293-320

[19] Kuznetsov S., Pospíšil S., and Král R., Climatic wind tunnel for wind engineering tasks, *Technical Transactions*, Vol. 12, *Civil Engineering*, 2-B, 2015, pp. 303-316

[20] Counihan J., An improved method of simulating an atmospheric boundary layer in a wind tunnel, *Atmospheric Environment*, Vol. 3, 1969, pp. 197-214

[21] Kozmar H., Truncated vortex generators for part-depth wind-tunnel simulations of the atmospheric boundary layer flow, *J. Wind. Eng. Ind. Aerodyn.*, Vol. 99, 2011, pp. 130-136

[22] Pieterse, J.E., Harms, T.M., CFD investigation of the atmospheric boundary layer under different thermal stability conditions, *J. Wind. Eng. Ind. Aerodyn*., Vol. 121, pp. 82-97, 2013.

[23] Nakayama, H., Takemi, T., Nagai, H., Large-eddy simulation of plume dispersion under various thermally stratified boundary layers, *Adv. Sci. Res*., Vol. 11, 2014, pp. 75-81

[24] Ohya, Y., Hashimoto, H., Ozono, S., A numerical study of a thermally stratified boundary layer under various stable conditions, *J. Wind. Eng. Ind. Aerodyn.*, Vol. 67–68, 1997, pp. 793-804

[25] Menter, F. R., Two-Equation Eddy-Viscosity Turbulence Models for Engineering Applications, *AIAA Journal*, Vol. 32 (8), 1994, pp. 1598-1605

[26] Zilitinkevich, S., and Baklanov, A., Calculation Of The Height Of The Stable Boundary Layer In Practical Applications, *Boundary-Layer Meteorology*, Vol. 105 (3), pp. 389-409. 2002